Internal Water Molecules of *pharaonis* Phoborhodopsin Studied by Low-Temperature Infrared Spectroscopy†

Hideki Kandori,*,‡ Yuji Furutani,‡ Kazumi Shimono,§ Yoshinori Shichida,‡ and Naoki Kamo§

Department of Biophysics, Graduate School of Science, Kyoto University, Sakyo-ku, Kyoto 606-8502, Japan, and Laboratory of Biophysical Chemistry, Graduate School of Pharmaceutical Sciences, Hokkaido University, Sapporo 060-0812, Japan

Received August 6, 2001; Revised Manuscript Received October 16, 2001

ABSTRACT: In the Schiff base region of bacteriorhodopsin (BR), a light-driven proton-pump protein, three internal water molecules are involved in a pentagonal cluster structure. These water molecules constitute a hydrogen-bonding network consisting of two positively charged groups, the Schiff base and Arg82, and two negatively charged groups, Asp85 and Asp212. Previous infrared spectroscopy of BR revealed stretching vibrations of such water molecules under strong hydrogen-bonding conditions using spectral differences in D_2O and $D_2{}^{18}O$ [Kandori and Shichida (2000) *J. Am. Chem. Soc. 122*, 11745−11746]. The present study extends the infrared analysis to another archaeal rhodopsin, *pharaonis* phoborhodopsin (*p*pR; also called *pharaonis* sensory rhodopsin-II, *p*sR-II), involved in the negative phototaxis of *Natronobacterium pharaonis*. Despite functional differences between *p*pR and BR, similar spectral features of water bands were observed before and after photoisomerization of the retinal chromophore at 77 K. This implies that the structure and the structural changes of internal water molecules are similar between *p*pR and BR. Higher stretching frequencies of the bridged water in *p*pR suggest that the water-containing pentagonal cluster structure is considerably distorted in *p*pR. These observations are consistent with the crystallographic structures of *p*pR and BR. The water structure and structural changes upon photoisomerization of ppR are discussed here on the basis of their infrared spectra.

Halobacteria contain four retinal proteins (archaeal rhodopsins): bacteriorhodopsin (bR)[1] (*1*, *2*), halorhodopsin (hR) (*3*, *4*), sensory rhodopsin (sR) (*5*−*7*), and phoborhodopsin (pR)[2] (*8*, *9*). bR and hR are light-driven ion pumps, which act as an outward proton pump and an inward Cl^- pump, respectively (*1*, *2*, *4*). sR and pR are photoreceptors of this bacterium, which act for attractant and repellent responses in phototaxis, respectively (*7*, *10*, *11*). These four retinal proteins are presumably evolved from the same protein, allowing them to specialize their functions (*12*). In fact, replacement of a single amino acid converts bR into a chloride ion pump like hR (*13*). In the absence of a transducer protein, sR can also act as a proton pump like bR (*14*).

Archaeal rhodopsins have similar structures: seven transmembrane helices and a retinal chromophore bound to a lysine residue of helix G via a protonated Schiff base linkage. To stabilize a positive charge of the Schiff base inside the protein, highly conserved charged groups are present in the Schiff base region: arginine and aspartate of helix C and aspartate of helix G. In hR, the aspartate of helix C is replaced to threonine (Thr111), while a chloride ion binds to the Schiff base region (*15*). The interaction of sR with the cognate transducer protonates the aspartate of helix C (Asp73), prohibiting proton transport (*14*). Thus, the Schiff base structure is directly linked to the functions of archaeal rhodopsins.

Water molecules also stabilize the charged groups in the Schiff base region. In fact, FTIR spectroscopy of bR using the isotope effect between H_2O and $H_2{}^{18}O$ (*16*, *17*) shows that water structural changes occur in the photocycle. The location of these water molecules was examined by using mutants in which this structure was perturbed (*16*, *17*). Subsequently, the crystal structure of BR (light-adapted bacteriorhodopsin having proton-pump activity) confirmed the location of several internal water molecules in the Schiff base region (*18*, *19*). In particular, three water molecules are involved in the pentagonal cluster structure, together with each oxygen of the negative charged Asp85 and Asp212. This pentagonal cluster also interacts with the positively charged Schiff base and Arg82. Thus, the water-containing cluster structure must play crucial role in stabilizing charged states of amino acids inside BR. In addition, internal water molecules may work to determine the vectoriality in BR during the "switching reaction" (*17*, *20*).

Despite extensive FTIR studies, the previous infrared spectroscopy observed water bands in a limited frequency

† This work was supported in part by grants from the Japanese Ministry of Education, Culture, Sports, Science, and Technology and by the Human Frontier Science Program.

* To whom correspondence should be addressed. Present address: Department of Applied Chemistry, Nagoya Institute of Technology, Showa-ku, Nagoya 466-8555, Japan. Phone and Fax: 81-52-735-5207. E-mail: kandori@ach.nitech.ac.jp.

‡ Kyoto University.

§ Hokkaido University.

[1] Abbreviations: bR, bacteriorhodopsin; hR, halorhodopsin; sR, sensory rhodopsin; pR, phoborhodopsin; *p*pR, *pharaonis* phoborhodopsin; BR, light-adapted bacteriorhodopsin that has *all-trans*-retinal as its chromophore; BR_K, K intermediate of BR; pR_K, K intermediate of *pharaonis* phoborhodopsin; FTIR, Fourier transform infrared; PC, L-α-phosphatidylcholine.

[2] sR and pR are also called sensory rhodopsin-I (sR-I) and sensory rhodopsin-II (sR-II), respectively.

10.1021/bi011621n CCC: $20.00
Published on Web 11/29/2001

region (*17*). A water molecule has two O−Hs, and their frequencies distribute in the wide 3700−2800 cm^{-1} region depending on their coupling and hydrogen-bonding strength (*21*), whereas only the water bands in the >3450 cm^{-1} had been discussed in the previous studies. The reason for the difficulty in identifying water O−H bands in the 3450−2800 cm^{-1} region is mainly owing to the spectral overlap of many bands from the protein and bulk waters. In addition, strongly hydrogen-bonded water possesses broad O−H stretches, which disturb the observation of clear isotope shifts. In fact, an isotope shift between O−H and ^{18}O−H is about 10 cm^{-1}, and such a small shift could be hidden in the complex spectral features of the 3450−2800 cm^{-1} region. However, this water cluster (*18*, *19*) requires more detailed FTIR study, particularly regarding the hydrogen bonds of the bridged water molecules in a very crowded part of the spectrum (*17*).

In 1998, we showed highly accurate difference spectra between BR_K and BR by means of low-temperature polarized FTIR spectroscopy (*22*). On the basis of this method, we attempted to observe stretching vibrations of the water molecules in their whole spectral region, using polarized FTIR spectroscopy with a BR film hydrated with D_2O or $D_2{}^{18}O$ (*23*). Examining the water stretching modes in D_2O had two advantages. One was that the D_2O-insensitive stretching vibrations were separated in frequency; the other was an expected isotope shift between O−D and ^{18}O−D of about 17 cm^{-1}, which is greater than that between O−H and ^{18}O−H (10 cm^{-1}). As a consequence, we successfully extended infrared analysis through the entire water stretching region (*23*). The observed frequencies were widely distributed over the possible stretching vibrations of water. Lower frequencies than those of fully tetrahedral water molecules implied that such water molecules in BR are hydrated with negatively charged Asp85 or Asp212. In addition, polarized measurement detected rotational motion of a dipole moment of a water molecule under strong hydrogen bonds, suggesting that the photoisomerization is accompanied by rotation of a water molecule hydrated with Asp85 or Asp212 (*23*).

In the present study, we extend the infrared analysis to another archaeal rhodopsin, *pharaonis* phoborhodopsin (*p*pR; also called *pharaonis* sensory rhodopsin-II, *p*sRII) (*10*, *11*). *p*pR mediates the negative phototaxis of *Natronobacterium pharaonis*. Upon absorption of a photon, *p*pR activates a cognate transducer protein during its photocycle. It was reported that *p*pR can pump a proton like BR in the absence of the transducer, whereas the pumping efficiency is much lower in *p*pR than in BR (*24*, *25*). These facts suggest a similar architecture of the protein between *p*pR and BR, which is also revealed by recent FTIR spectroscopy of *p*pR (*26*). However, this raises several questions. Do water molecules in *p*pR hydrate negatively charged aspartates such as BR? How many water molecules change their hydrogen bonds with retinal photoisomerization? This study shows the presence of water molecules hydrated with negatively charged groups. Spectral changes of water bands before and after photoisomerization of the retinal chromophore were essentially similar between *p*pR and BR. On the other hand, higher frequencies of the bridged water stretches in *p*pR suggest that the water-containing pentagonal cluster structure is considerably distorted in *p*pR.

MATERIALS AND METHODS

The *p*pR sample was prepared as described previously (*26*). Briefly, the *p*pR protein having a histidine tag at the C-terminus was expressed in *Escherichia coli*, solubilized with 1.5% *n*-dodecyl β-D-maltoside (DM), and purified by a Ni column. The purified *p*pR sample was then reconstituted into L-α-phosphatidylcholine (PC) liposomes by dialysis, where the molar ratio of the added PC was 50 times that of *p*pR.

FTIR spectroscopy was applied as described previously (*23*, *26*, *27*). Eighty microliters of the *p*pR sample in 2 mM phosphate buffer (pH 7.0) was dried on a BaF_2 window with a diameter of 18 mm. After hydration by H_2O, D_2O, or $D_2{}^{18}O$, the sample was mounted in an Oxford DN-1704 cryostat and cooled to 77 K. Illumination with 450 nm light converted *p*pR to pR_K, and subsequent illumination with >560 nm light reverted pR_K to *p*pR. The difference spectrum was calculated from the spectra constructed with 128 interferograms before and after the illumination. Twenty-four spectra obtained in this way were averaged for the pR_K minus *p*pR spectrum. Linear dichroism experiments revealed a random orientation of the *p*pR molecules in the film. Therefore, an IR polarizer was not used in the measurements for *p*pR.

RESULTS AND DISCUSSION

Spectral Changes of ppR in the High-Frequency Region. Figure 1 shows the pR_K minus *p*pR spectra for a hydrated film with H_2O (a) and D_2O (b) in the 3800−1750 cm^{-1} region. Spectral features in the lower frequency region (1750−740 cm^{-1}) (data not shown) were identical to those reported previously (*26*). Figure 1a shows a broad negative band at 3000−2300 cm^{-1}. A similar negative band was observed in the BR_K minus BR spectrum (*22*), although it was located at a higher frequency (3100−2700 cm^{-1}) than that for *p*pR. On the other hand, sharp peaks are observed at >3450 cm^{-1}, characteristic of O−H stretching vibrations of water molecules under weak hydrogen bonds (*17*).

Figure 1b shows both D_2O-insensitive and D_2O-sensitive bands at 3700−2700 and 2700−1900 cm^{-1}, respectively. In general, the former is composed of O−H, N−H, and C−H stretches, while the latter is composed of O−D and N−D stretches. The broad negative feature at 3000−2300 cm^{-1} in H_2O (Figure 1a) is shifted to the lower frequency side in D_2O, exhibiting various negative peaks at 2307, 2215, 2142, 2090, and 2007 cm^{-1} (Figure 1b). In addition, the X−H stretches at 3660 (−), 3653 (+), 3626 (−), 3619 (+), 3538 (+), and 3480 (−) cm^{-1} in H_2O (Figure 1a) are likely to downshift to 2704 (−), 2700 (+), 2677 (−), 2672 (+), 2614 (+), and 2575 (−) cm^{-1} in D_2O, respectively (Figure 1b). Note that the infrared spectrum in D_2O (Figure 1b) is much more structured than the one in H_2O (Figure 1a) in the 3500−3100 cm^{-1} region. This is probably because of a spectral mixture of both D_2O-sensitive and -insensitive bands. In fact, subtraction of the spectrum in D_2O (Figure 1b) from that in H_2O (Figure 1a) in the 3700−3100 cm^{-1} region essentially coincides in shape with the spectrum in D_2O (Figure 1b) in the 2700−2300 cm^{-1} region (data not shown). A similar observation was obtained for BR (*22*).

The N−H stretching vibrations of the peptide backbone (amide-A) appear at 3320−3270 cm^{-1}, where amide-A

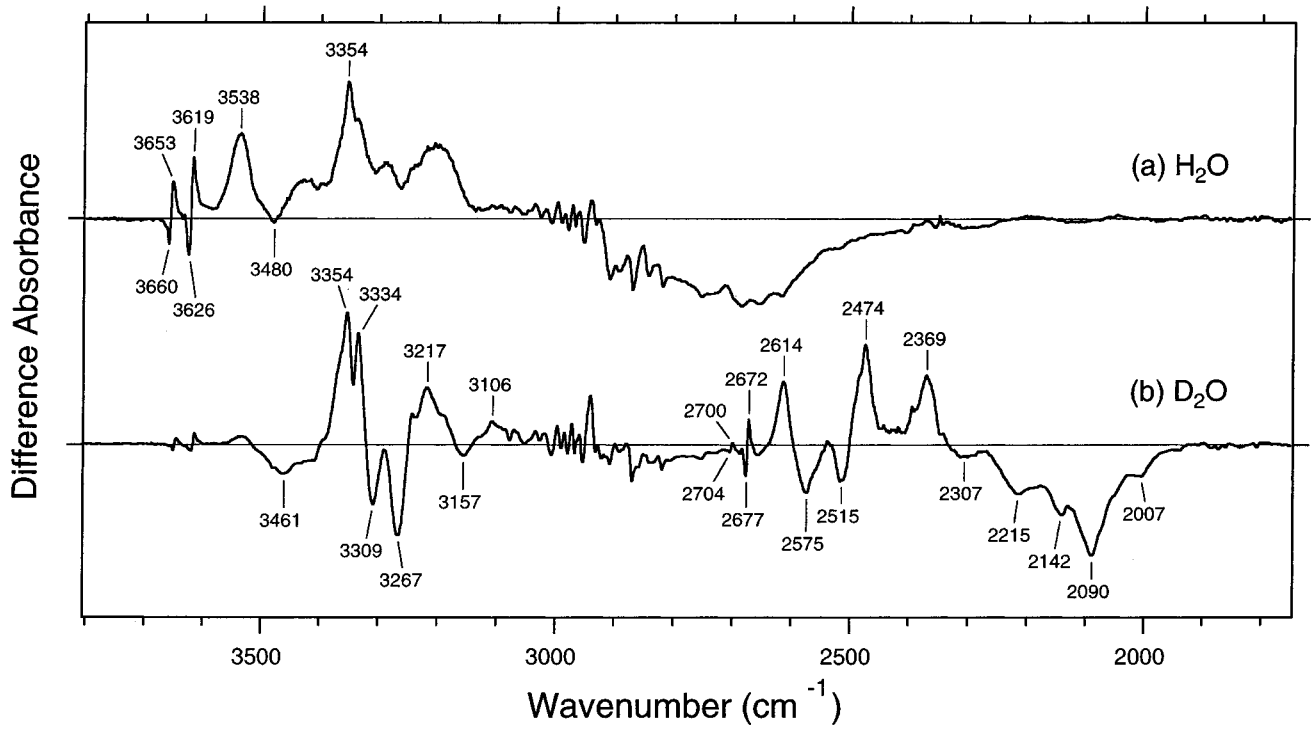

FIGURE 1: Difference infrared spectra of *p*pR measured at 77 K in the 3800−1750 cm^{-1} region. The sample was hydrated with H_2O (a) or D_2O (b). One division of the *Y*-axis corresponds to 0.002 absorbance unit.

vibrations in the α-helix are located at 3279 cm^{-1} (*28*). Therefore, sharp peaks at 3334 (+), 3309 (−), and 3267 (−) cm^{-1} in D_2O (Figure 1b) probably correspond to amide-A vibrations. We previously observed peaks at 1671 (+), 1662 (−), and 1658 (−) cm^{-1} in the frequency region of C═O stretching vibrations of the peptide backbone (amide-I) (*26*). Since the frequency at 1658 cm^{-1} corresponds to characteristic amide-I vibration of the α-helix, the N−H group at 3267 cm^{-1} is likely to form a hydrogen bond with the C═O group at 1658 cm^{-1} in *p*pR. On the other hand, it is known that amide-A and amide-I vibrations are considerably upshifted in the distorted α-helix (called αII-helix) (*29*). Thus, the amide-A vibrations at 3334 (+)/3309 (−) cm^{-1} are likely to correspond to the amide-I vibrations at 1671 (+)/1662 (−) cm^{-1}, which probes structural changes in the αII-helix. Higher frequency shift in the αII-helix upon formation of pR_K indicates weakened hydrogen bond. This observation is in contrast to that for BR, where lower frequency shifts were observed for both amide-A and amide-I vibrations of the αII-helix (*22*).

Water Structural Changes in ppR and Its Comparison with BR. Figure 2 shows a spectral comparison between hydration with D_2O (solid lines) and $D_2{}^{18}O$ (dotted lines) for *p*pR (a) and BR (b). Linear dichroism measurements revealed that *p*pR molecules are randomly oriented in the hydrated film, while BR molecules are highly oriented (*26*). Therefore, we made dichroic measurements of the hydrated film of BR with an IR polarizer. The spectra in Figure 2b are reproduced from ref *23*, where the IR window was tilted by 53.5°.

In BR, at least five peaks were assigned to the O−D stretching vibrations of water molecules, where frequencies are widely distributed over the possible stretching vibrations of water (Figure 2b). Since the frequencies of the negative peaks at 2292 and 2171 cm^{-1} are much lower than those of the fully hydrated tetrahedral water molecules (*23*, *30*, *31*), the hydrogen bonds of these water molecules are very strong, possibly associated with negative charges. We tentatively assigned the hydrogen-bonding acceptors of these water O−D stretches as the negatively charged oxygens of Asp85 and Asp212 (*23*). The water stretching vibrations of BR_K tend to be higher in frequency, implying that the overall hydrogen bonding becomes weaker upon photoisomerization. In addition, it was found that the dipole moments of the water O−D stretches in BR are generally parallel to the membrane, while that of the 2265 cm^{-1} band of BR_K (Figure 2b) is parallel to the membrane normal. This observation suggests that photoisomerization is accompanied by rotation of a water molecule (*23*).

Spectral comparison between hydration with D_2O and $D_2{}^{18}O$ for *p*pR clearly demonstrates an isotope shift of water molecules in the wide region. The peaks at 2704 (−), 2700 (+), 2677 (−), 2672 (+), 2614 (+), and 2575 (−) cm^{-1} in D_2O were shifted to those at 2688 (−), 2683 (+), 2661 (−), 2656 (+), 2598 (+), and 2559 (−) cm^{-1} in $D_2{}^{18}O$, respectively. Shifts by 16−17 cm^{-1} are consistent with the expected isotope shift (17 cm^{-1}). Thus, all of the spectral changes of *p*pR in the 2740−2550 cm^{-1} region originate from the O−D stretches of weakly hydrogen-bonded water molecules (Figure 2a). A similar result was obtained for BR (Figure 2b).

The O−D stretches at 2690 (−)/2684 (+) cm^{-1} in BR correspond to the O−H stretches at 3643 (−)/3636 (+) cm^{-1}, which are almost free from hydrogen bonding. *p*pR exhibits two peak pairs at such frequencies; 3660 (−)/3653 (+) cm^{-1} and 3626 (−)/3619 (+) cm^{-1} as water O−H stretches, shifting to 2704 (−)/2700 (+) cm^{-1} and 2677 (−)/2672 (+) cm^{-1} in D_2O, respectively. A water molecule in a protein tends to form at least one hydrogen bond between the two O−H groups, which is the case in BR (*17*). It is thus likely that in *p*pR there are two water molecules possessing O−D

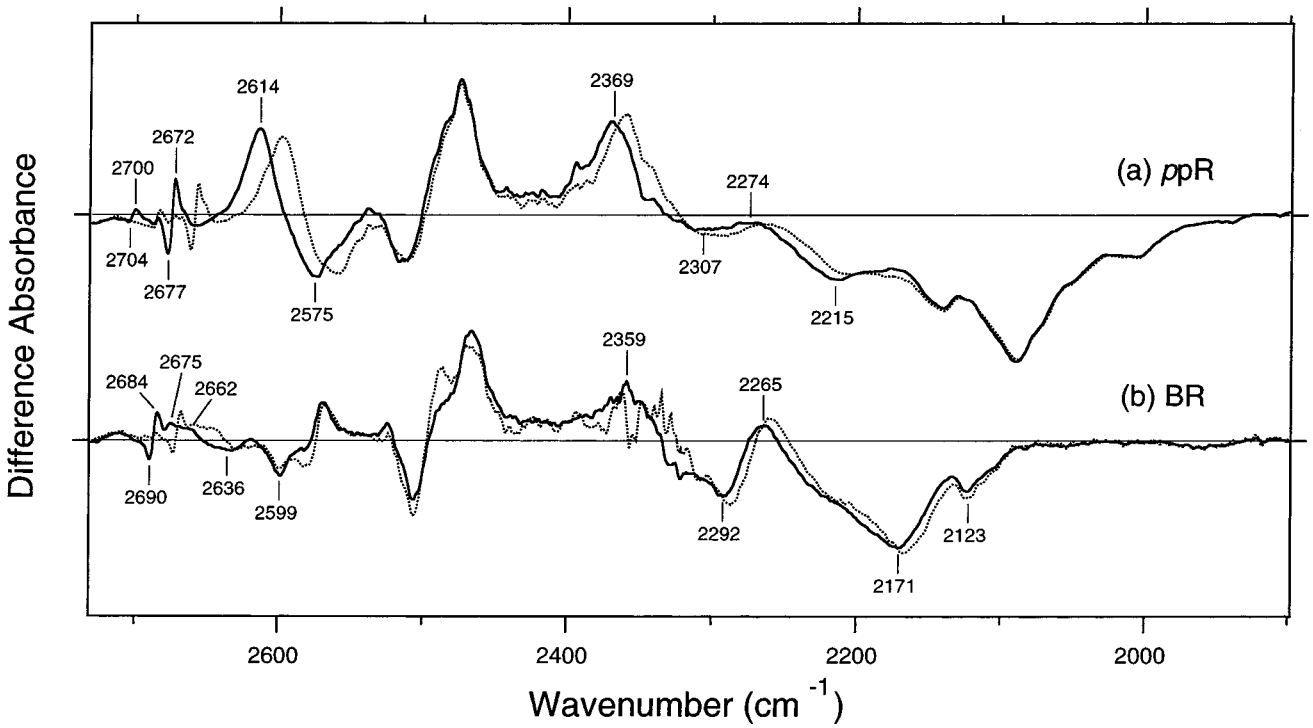

FIGURE 2: ppR_K minus *pp*R (a) and BR_K minus BR (b) spectra in the 2730−1900 cm^{-1} region. The sample was hydrated with D_2O (solid lines) or $D_2{}^{18}O$ (dotted lines). In the hydrated film, *pp*R molecules are randomly oriented, while BR molecules are highly oriented. Spectra in (b) are reproduced from ref *23*, where the sample window is tilted by 53.5°. One division of the *Y*-axis corresponds to 0.0015 absorbance unit.

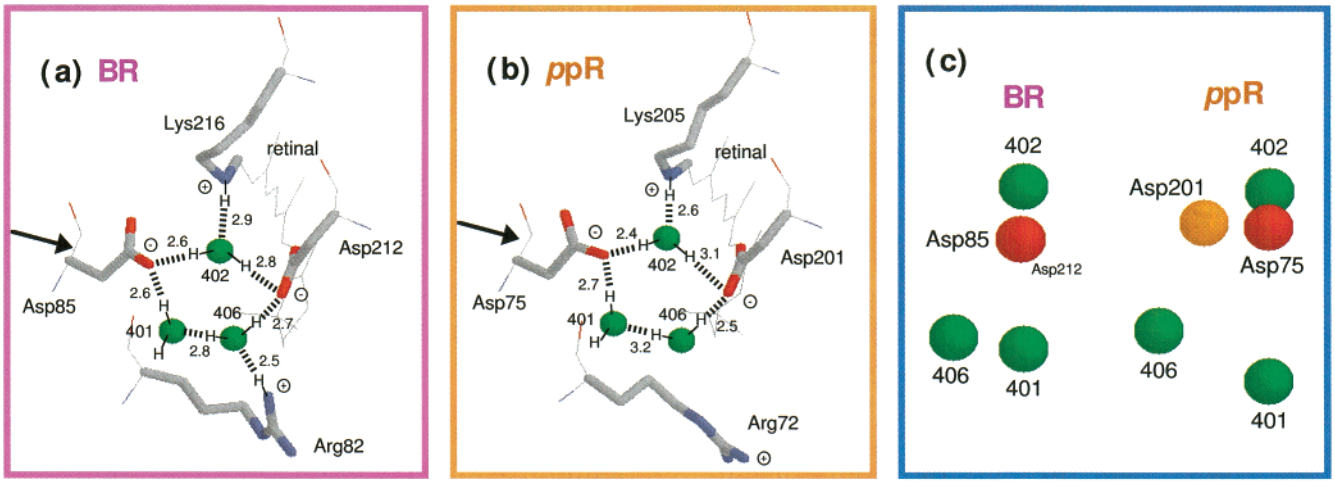

FIGURE 3: Diffraction structures of the Schiff base region in BR (a) and *pp*R (b), which are the side view of 1C3W (*18*) and 1JGJ (*35*), respectively. The coordinate of *pp*R is a gift from Dr. H. Luecke before its release. The membrane normal is approximately in the vertical direction of this figure. Upper and lower regions correspond to the cytoplasmic and extracellular sides, respectively. The peptide backbone and retinal molecule are shown by a wireframe drawing, while side chains are shown by a stick drawing. Green circles (401, 402, and 406) represent water molecules in the Schiff base region. Dotted lines represent supposed hydrogen bonds, and numbers are O−O or O−N distances in angstroms. (c) Atomic positions of the pentagonal cluster in BR (left) and *pp*R (right) viewed along the arrow in (a) and (b), respectively. In BR, two oxygen atoms of Asp85 and Asp212 are overlapped, so that the oxygen of Asp212 is hidden.

(O−H) stretches free from hydrogen bonding that experience frequency changes upon photoisomerization of the retinal chromophore. In addition, a large peak pair at 2614 (+)/2575 (−) cm^{-1} is prominent for *pp*R. The band could be composed of multiple O−D stretches of water.

The peaks at 2515 (−)/2474 (+) cm^{-1} of *pp*R did not exhibit an isotope shift for water molecules (Figure 2a). Similar observations were seen for the 2506 (−)/2466 (+) cm^{-1} bands of BR, which were previously assigned as the O−D stretch of Thr89 (*32*). Therefore, the 2515 (−)/2474 (+) cm^{-1} bands of *pp*R possibly originate from the O−D stretch of Thr79 (*26*). Future analysis will identify these bands. Note that the isotope-induced spectral deviation was reproducible in the frequency region for BR (Figure 2b), suggesting that the water O−D stretch is involved in this frequency region. In contrast, identical spectra in D_2O and $D_2{}^{18}O$ indicate that there are no water bands in this region in *pp*R (Figure 2a).

The hydrogen bond of the water O−D stretch at <2400 cm^{-1} is stronger than that of a fully hydrated tetrahedral water, suggesting that the O−D group is hydrated with a negative charge (*23*). All peaks in the 2400−2200 cm^{-1}

region of *p*pR exhibited spectral downshifts by about 10 cm^{-1} (Figure 2a), indicating that the spectral changes in this region originate from the O−D stretches of water molecules. Thus, the O−D stretches at 2307 and 2215 cm^{-1} are likely to be hydrated with negative charges in *p*pR. Note that the spectral feature in this region looks similar between *p*pR and BR, while peak frequencies are higher in *p*pR. In BR, peaks in the wider 2400−2150 cm^{-1} region exhibited isotope shifts of water (Figure 2b). In both *p*pR and BR, higher frequency shifts upon K formation suggest that hydrogen bonds with negative charges are weakened upon photoisomerization.

The 2274 cm^{-1} band of *p*pR (Figure 2a) does not appear in the positive side, and the corresponding 2265 cm^{-1} band of BR is highly dichroic (*23*). In an oriented film of BR, there is no positive band at 2265 cm^{-1} without tilting the sample film (*23*), while there is a positive peak at 2265 cm^{-1} when the sample film is tilted at 53.5° (Figure 2b). This result indicates that the O−D stretch mode is parallel to the membrane normal. Since no water bands have the O−D stretches parallel to the membrane normal before photoisomerization (BR state), this observation provided experimental evidence of the rotation of a water molecule (*23*). It is interesting to determine if the 2274 cm^{-1} band of *p*pR has a dipole moment parallel to the membrane normal. *p*pR molecules are randomly oriented in the present sample film. Dichroic measurement to the highly oriented *p*pR film will answer this question.

Peaks at 2142, 2090, and 2007 cm^{-1} in *p*pR (Figure 1b) do not originate from the water O−D stretches (Figure 2a). The bands correspond to the broad negative feature in the 2800−2500 cm^{-1} region (Figure 1). In the case of BR, only the negative band at 2123 cm^{-1} does not originate from the water O−D stretch (Figure 2b). According to the literature, strongly hydrogen-bonded N−H groups can possess their stretching frequencies at $<$3200 cm^{-1} (*33*), which corresponds to $<$2400 cm^{-1} for the N−D stretches. Therefore, the N−D stretches of the Schiff base and arginine are candidates. Previous resonance Raman (*34*) and FTIR (*26*) studies showed from the analysis of the C=N stretch in H_2O and D_2O that the hydrogen-bonding strength of the Schiff base is stronger in *p*pR than in BR. In addition, FTIR studies suggested that the hydrogen bond of the Schiff base in *p*pR is weakened upon photoisomerization like BR (*26*). From these facts, we can expect that the N−D stretch of the Schiff base in *p*pR is lower in frequency than in BR, and photoisomerization accompanies higher frequency shifts in both *p*pR and BR. In this sense, the negative bands at 2090 cm^{-1} in *p*pR and 2123 cm^{-1} in BR are good candidates for the Schiff base vibration. The N−D stretch of arginine is an alternative candidate, where more negative bands at 2142, 2090, and 2007 cm^{-1} in *p*pR (Figures 1b and 2a) might suggest greater changes in the Arg72 of *p*pR than in the Arg82 of BR. Isotope labels of lysine and arginine will assign these vibrational bands in the future.

In summary, *p*pR exhibited five peaks of water O−D stretches in the difference spectrum between the original state and the K intermediate. The results imply that at least three water molecules change their hydrogen bonds accompanying photoisomerization of the retinal chromophore in *p*pR, as is in BR (*23*). In addition, wide distribution of water O−D stretches in *p*pR was also similar to that in BR. These facts suggest similarities between the internal water molecules in *p*pR and BR. In fact, water O−D stretches hydrating with negative charges were observed in *p*pR as well as in BR, although higher frequencies of the bridged water stretches in *p*pR suggest that the water-containing pentagonal cluster structure is considerably distorted in *p*pR.

Structure of the Schiff Base Region in ppR and BR. Figure 3a shows the structure of the Schiff base region in BR. Three water molecules (Waters 401, 402, and 406) are involved in the pentagonal cluster structure together with each oxygen of the negative charged Asp85 and Asp212. The pentagonal cluster also interacts with the positively charged Schiff base and Arg82 (Figure 3a). Specific frequencies and dipolar orientations provided insight into the water structures and their structural changes in BR. Water molecules associating with Asp85 or Asp212 presumably possess an O−D stretch at $<$2400 cm^{-1}, one of which rotates upon photoisomerization of the retinal chromophore (*23*).

Although the structure of *p*pR was not known during our studies, a X-ray crystallographic structure of *p*pR has appeared during the writing of this paper (*35*).[3] Figure 3b shows the structure of the Schiff base region in *p*pR. Despite different absorption properties between *p*pR and BR, the structure looks similar. In particular, the pentagonal cluster structure is preserved in the Schiff base region of *p*pR (Figure 3b). Thus, the water O−D stretches of *p*pR at 2307 and 2215 cm^{-1} (Figure 2a) presumably originate from those associating with negatively charged Asp75 and/or Asp201.

As is suggested by the infrared spectra, the pentagonal cluster structure is more distorted in *p*pR than in BR. In fact, the five hydrogen-bonding distances within the pentagonal cluster are 2.6−2.8 Å in BR (Figure 3a) and 2.4−3.2 Å in *p*pR (Figure 3b). In addition, the pentagonal cluster is more planer in BR than in *p*pR (Figure 3c). It is intriguing that the closest hydrogen bond of water in BR (2.6 Å; Figure 3a) is longer than that in *p*pR (2.4 Å; Figure 3b), whereas the hydrogen bond of water is stronger in BR (2171 cm^{-1}; Figure 2b) than in *p*pR (2215 cm^{-1}; Figure 2a) in view of vibrational frequencies. The reason is unclear at present. The current resolution of the X-ray crystallography may not be sufficient to compare such small differences in distance. On the other hand, stronger vibrational coupling inside the pentagonal cluster in BR might lower O−D stretching frequencies. In fact, recent ab initio QM/MM calculations revealed that the vibrational modes of the water O−D and the Schiff base N−D stretches are highly sensitive to vibration−electron coupling (*36*). Involvement of Arg82 in the hydrogen-bonding network in BR, but not in *p*pR, could be also correlated with the present observation.

The X-ray structure of *p*pR also revealed that the other water molecules in BR are preserved in *p*pR, such as Waters 407, 501, 501, and 511 (named 602 in *p*pR) (*35*; not shown). Thus, the widely distributed water bands in *p*pR as in BR (Figure 2) are possibly contributed by these water molecules. In contrast, *p*pR has a unique water molecule near Trp76 and Tyr174 (*35*), whereas BR does not have such water at the corresponding position. It is possibly related to the intense bands at 2614 (+)/2575 (−) cm^{-1}.

[3] Another group has independently reported the structure of *p*pR (*37*) (Protein Data Bank: 1H68). The two structures are very similar, particularly in regard to the pentagonal cluster structure.

In conclusion, association of water molecules to the negatively charged aspartates (Asp75 and/or Asp201) was evident from our infrared spectroscopy, and these observations were also supported by the recent X-ray crystallographic structure (*35*). In addition, infrared spectral comparisons revealed that the hydrogen bonds are weaker in *p*pR than in BR, suggesting that the water-containing hydrogen-bonding network is distorted in *p*pR. Water structural changes after photoisomerization of the retinal chromophore are similar in *p*pR to those in BR, where perturbation on the hydrogen-bonding network leads to proton transfer upon M formation.

ACKNOWLEDGMENT

We thank Masayuki Iwamoto and Yuki Sudo for help in the preparation of the *p*pR samples. We are grateful to Dr. H. Luecke for the generous gift of the coordinates of *p*pR (1JGJ) before its release.

REFERENCES

1. Lanyi, J. K. (1997) *J. Biol. Chem. 272*, 31209−31212.
2. Haupts, U., Tittor, J., and Oesterhelt, D. (1999) *Annu. Rev. Biophys. Biomol. Struct. 28*, 367−399.
3. Matsuno-Yagi, A., and Mukohata, Y. (1977) *Biochem. Biophys. Res. Commun. 78*, 237−243.
4. Lanyi, J. K. (1990) *Physiol. Rev. 70*, 319−330.
5. Bogomolni, R. A., and Spudich, J. L. (1982) *Proc. Natl. Acad. Sci. U.S.A. 79*, 6250−6254.
6. Tsuda, M., Hazemoto, N., Kondo, M., Kamo, N., Kobatake, Y., and Terayama, Y. (1982) *Biochem. Biophys. Res. Commun. 108*, 970−976.
7. Hoff, W. D., Jung, K. H., and Spudich, J. L. (1997) *Annu. Rev. Biophys. Biomol. Struct. 26*, 223−258.
8. Takahashi, T., Tomioka, H., Kamo, N., and Kobatake, Y. (1985) *FEMS Microbiol. Lett. 28*, 161−164.
9. Zhang, W., Brooun, A., Mueller, M. M., and Alam, M. (1996) *Proc. Natl. Acad. Sci. U.S.A. 93*, 8230−8235.
10. Sasaki, J., and Spudich, J. L. (2000) *Biochim. Biophys. Acta 1460*, 230−239.
11. Kamo, N., Shimono, K., Iwamoto, M., and Sudo, Y. (2001) *Biochemistry (Moscow)* (in press).
12. Ihara, K., Umemura, T., Katagiri, I., Kitajima-Ihara, T., Sugiyama, Y., and Mukohata, Y. (1999) *J. Mol. Biol. 285*, 163−174.
13. Sasaki, J., Brown, L. S., Chon, Y.-S., Kandori, H., Maeda, A., Needleman, R., and Lanyi, J. K. (1995) *Science 269*, 73−75.
14. Bogomolni, R. A., Stoeckenius, W., Szundi, I., Perozo, E., Olson, K. D., and Spudich, J. L. (1994) *Proc. Natl. Acad. Sci. U.S.A. 91*, 10188−10192.
15. Kolbe, M., Besir, H., Essen, L. O., and Oesterhelt, D. (2000) *Science 288*, 1390−1396.
16. Maeda, A., Kandori, H., Yamazaki, Y., Nishimura, S., Hatanaka, M., Chon, Y.-S., Sasaki, J., Needleman, R., and Lanyi, J. K. (1997) *J. Biochem. 121*, 399−406.
17. Kandori, H. (2000) *Biochim. Biophys. Acta 1460*, 177−191.
18. Luecke, H., Schobert, B., Richter, H.-T., Cartailler, J. P., and Lanyi, J. K. (1999) *J. Mol. Biol. 291*, 899−911.
19. Belrhali, H., Nollert, P., Royant, A., Menzel, C., Rosenbusch, J. P., Landau, E. M., and Pebay-Peyroula, E. (1999) *Structure 7*, 909−917.
20. Luecke, H. (2000) *Biochim. Biophys. Acta 1460*, 133−156.
21. Eisenburg, D., and Kauzmann, W. (1969) *The Structure and Properties of Water*, Oxford Press, London.
22. Kandori, H., Kinoshita, N., Shichida, Y., and Maeda, A. (1998) *J. Phys. Chem. B 102*, 7899−7905.
23. Kandori, H., and Shichida, Y. (2000) *J. Am. Chem. Soc. 122*, 11745−11746.
24. Schmies, G., Luttenberg, B., Chizhov, I., Engelhard, M., Becker, A., and Bamberg, E. (2000) *Biophys. J. 78*, 959−966.
25. Sudo, Y., Iwamoto, M., Shimono, K., Sumi, M., and Kamo, N. (2001) *Biophys. J. 80*, 916−922.
26. Kandori, H., Shimono, K., Sudo, Y., Iwamoto, M., Shichida, Y., and Kamo, N. (2001) *Biochemistry 40*, 9238−9246.
27. Kandori, H., and Maeda, A. (1995) *Biochemistry 34*, 14220−14229.
28. Krimm, S., and Bandekar, J. (1986) *Adv. Protein Chem. 38*, 181−364.
29. Krimm, S., and Dwivedi, A. M. (1982) *Science 216*, 407−408.
30. Monosmith, W. B., and Walrafen, G. E. (1984) *J. Chem. Phys. 15*, 660−674.
31. Walrafen, G. E., and Fisher, M. R. (1986) *Methods Enzymol. 127*, 91−105.
32. Kandori, H., Kinoshita, N., Yamazaki, Y., Maeda, A., Shichida, Y., Needleman, R., Lanyi, J. K., Bizounok, M., Herzfeld, J., Raap, J., and Lugtenburg, J. (1999) *Biochemistry 38*, 9676−9683.
33. Lin-Vien, D., Colthup, N. B., Fateley, W. G., and Grasselli, J. G. (1991) *The Handbook of Infrared and Raman Characteristic Frequencies of Organic Molecules*, Academic Press, San Diego.
34. Gellini, C., Jüttenberg, B., Sydor, J., Engelhard, M., and Hildebrandt, P. (2000) *FEBS Lett. 472*, 263−266.
35. Luecke, H., Schobert, B., Lanyi, J. K., Spudich, E. N., and Spudich, J. L. (2001) *Science 293*, 1499−1503.
36. Hayashi, S., and Ohmine, I. (2000) *J. Phys. Chem. B 104*, 10678−10691.
37. Royant, A., Nollert, P., Edman, K., Nuetze, R., Landau, E. M., Pebay-Peyroula, E., and Navarro, J. (2001) *Proc. Natl. Acad. Sci. U.S.A. 98*, 10131−10136.

BI011621N